Supporting Information for **“[Gd(Try-TTDA)(H_2O)]$^{2-}$: A new MRI contrast agent for copper ion sensing** ”

Dayananda Kasala,[a,b] Tsung-Sheng Lin,[a] Chiao-Yun Chen[c,d] Gin-Chung Liu,[c,d] Chai-Lin Kao,[e] Tian-Lu Cheng,[f] Yun-Ming Wang[a,b]*

*Corresponding author. E-mail address: ymwang@mail.nctu.edu.tw

Variable-temperature ^{17}O NMR measurements.

For the ^{17}O NMR measurements, the inversion recovery method was applied to measure longitudinal relaxation rates, $1/T_1$, and the Carr-Purcell-Meiboom-Gill spin-echo technique was used to obtain transverse relaxation rates, $1/T_2$. In order to eliminate magnetic susceptibility corrections to chemical shift, the solution was introduced into spherical glass containers fitting into ordinary 10-mm NMR tubes. From the measured ^{17}O NMR relaxation rates and angular frequencies of the Gd(III) containing solutions, $1/T_1$, $1/T_2$, and ω, and of the acidified water reference, $1/T_{1A}$, $1/T_{2A}$, and ω_A, one can calculate the reduced relaxation rates and chemical shift, $1/T_{1r}$, $1/T_{2r}$, and $\Delta\omega_r$ (Fig. 3)(Tables S2 and 2):

$$\frac{1}{T_{1r}} = \frac{1}{P_m}\left[\frac{1}{T_1} - \frac{1}{T_{1A}}\right] = \frac{1}{T_{1m} + \tau_m} + \frac{1}{T_{1os}} \qquad (1S)$$

$$\frac{1}{T_{2r}} = \frac{1}{P_m}\left[\frac{1}{T_2} - \frac{1}{T_{2A}}\right] = \frac{1}{\tau_m}\frac{T_{2m}^{-2} + \tau_m^{-1}T_{2m}^{-1} + \Delta\omega_m^2}{\left(\tau_m^{-1} + T_{2m}^{-1}\right)^2 + \Delta\omega_m^2} + \frac{1}{T_{2os}} \qquad (2S)$$

$$\Delta\omega_r = \frac{1}{P_m}(\omega - \omega_A) = \frac{\Delta\omega_m}{\left(1 + \tau_m T_{2m}^{-1}\right)^2 + \tau_m^2\Delta\omega_m^2} + \Delta\omega_{os} \qquad (3S)$$

P_m is the mole fraction of bound water.

$1/T_{2m}$ is the relaxation rates in the bound water.

$\Delta\omega_m$ is the chemical shift difference between bound water and bulk water.

$$\Delta \omega_m = \frac{g_L \mu_B S(S+1)B}{3k_B T} \frac{A}{\hbar} \qquad (4S)$$

where g_L is the isotropic Landé g factor ($g_L = 2.0$ for Gd(III))

S is the electron spin ($S = 7/2$ for Gd(III))

$A/\hbar$ is the hyperfine or scalar coupling constant

B is the magnetic field

$$\frac{1}{T_{2m}} \cong \frac{1}{T_{2sc}} = \frac{S(S+1)}{3}\left(\frac{A}{\hbar}\right)^2 \left[\tau_{1S} + \frac{\tau_{2S}}{1+\omega_S^2 \tau_{2S}^2}\right] \qquad (5S)$$

where $1/\tau_{is} = 1/\tau_M + 1/T_{ie}$

$\Delta H^{\neq}$ and $\Delta S^{\neq}$ are the enthalpy and entropy of activation for the exchange process:

$$\frac{1}{\tau_m} = k_{ex} = \frac{k_B T}{h} \exp\left\{\frac{\Delta S^*}{R} - \frac{\Delta H^*}{RT}\right\} \qquad (6S)$$

The ^{17}O longitudinal relaxation rates in Gd(III) solutions are dominated by the dipole-dipole and quadrupolar mechanisms, and are given by below :

$$\frac{1}{T_{1m}} = \left[\frac{1}{15}\left(\frac{\mu_0}{4\pi}\right)^2 \frac{\hbar^2 \gamma_I^2 \gamma_S^2}{r_{GdO}^6} S(S+1)\right]\left[6\pi_{d1} + 14\frac{\tau_{d2}}{1+\omega_S^2 \tau_{d2}}\right] + \frac{3\pi^2}{10}\frac{2I+3}{I^2(2I-1)}\chi^2\left(1+\frac{\eta^2}{3}\right)\tau_R \qquad (7S)$$

where γ_I is the nuclear gyromagnetic ratio ($\gamma_I = -3.626 \times 10^7$ rad $s^{-1}T^{-1}$ for ^{17}O), γ_{GdO} is the mean Gd(III)–O distance, I is the nuclear spin ($I = 5/2$ for ^{17}O), χ is the quadrupolar coupling constant, η an asymmetry parameter, and $\tau_{di} = \tau_M^{-1} + T_{ie}^{-1} + \tau_R^{-1}$. Using the quadrupolar coupling constant for acidified water, $\chi(1 + \eta^{2/3})^{1/2} = 7.58$ MHz, and estimating $r = 2.5$ Å is based on $[\mathrm{Gd(DTPA)}]^{2-}$ crystal structure.[1, 2]

$$\tau_R = \tau_R^{298} \exp\left[\frac{E_R}{R}\left(\frac{1}{T} - \frac{1}{298.15}\right)\right] \qquad (8S)$$

E_R : activation energy

The outer-sphere contribution to $\Delta\omega_\mathrm{r}$ has a similar temperature dependence to $\Delta\omega_\mathrm{m}$ and is given by below, where C_os is an empirical constant.

$$\Delta\omega_\mathrm{os} = C_{os}\Delta\omega_\mathrm{m} \qquad (9S)$$

Data analysis.

The simultaneous least-squares fitting of ^{17}O NMR data was determined by fitting the experimental data using the program *SCIENTIST®* for WINDOWS™ by *MICROMATH®*, version 2.0.

Conditional binding constant (K_d)

Fluorescence spectra of $[Gd(Try\text{-}TTDA)(H_2O)]^{2-}$ (200 μM) in acetate buffer, pH 5.5, with excitation at 280 nm show an emission maximum at 360 nm that decreases upon titration of $CuCl_2$. The fluorescence was quenched completely after addition of 1.0 equivalent as depicted in Figure S9. The conditional binding constant was obtained from equation 10S which relates fluorescence intensity to the concentration of Cu(II)[3]

$$(F_0 - F) / (F - F_\infty) = ([Cu^{2+}] / K_d)^n \qquad (10S)$$

where F_0, F and F_∞ are the relative fluorescence intensities of $[Gd(Try\text{-}TTDA)(H_2O)]^{2-}$, $[Gd(Try\text{-}TTDA)(H_2O)]^{-}$ in the presence of a know concentration of Cu^{2+}, $[Gd(Try\text{-}TTDA)(H_2O)]^{2-}$ saturated with Cu^{2+}, respectively and n is the equivalents of binding sites on $[Gd(Try\text{-}TTDA)(H_2O)]^{2-}$. By plotting log $[(F_0 - F) / (F - F_\infty)]$ vs log $[Cu^{2+}]$, the slope of line is equal to n and log (K_d) is equal to log (Cu^{2+}) where log $[(F_0 - F) / (F - F_\infty)] = 0$. Figure S9 shows a typical plot of log $[(F_0 - F) / (F - F_\infty)]$ vs log $[Cu^{2+}]$ for $[Gd(Try\text{-}TTDA)(H_2O)]^{2-}$, which gives an apparent K_d for $[Gd(Try\text{-}TTDA)(H_2O)]^{2-}$-Cu(II) complex of 2.52 mM.

References

1. M. R. Spirlet, J. Rebizant, J. F. Desreux, M. F. Loncin, *Inorg. Chem.* 1984, **23**, 359-363
2. J. J. Stezowski, J. L. Hoard, *Isr. J. Chem.* 1984, **24,** 323-334
3. K. C. Ciesienski, L. Y. Hyman, S. Derisavifard, K. J. Franz, *Inorg. Chem.*, 2010, **49**, 6808–6810.

Table S1 Luminescence lifetimes of $[Eu(Try\text{-}TTDA)(H_2O)]^{2-}$ and $[Eu(Try\text{-}ac\text{-}DOTA)(H_2O)]^{-}$ in the presence and absence of Cu (II) at room temperature.

Complexes	τ_{H2O}/ms	τ_{D2O}/ms	q^{a}
$[Eu(Try\text{-}TTDA)(H_2O)]^{2-}$	0.50	1.38	1.23
$[Eu(Try\text{-}TTDA)(H_2O)]^{2-}$+ Cu(II)	0.18	0.26	1.94
$[Eu(Try\text{-}ac\text{-}DOTA)(H_2O)]^{-}$	0.55	1.56	1.11
$[Eu(Try\text{-}ac\text{-}DOTA)(H_2O)]^{-}$ + Cu(II)	0.50	1.66	1.08

[a] $q= 1.2(k_{H2O}\text{-}k_{D2O}\text{-}\ 0.25)$

Table S2. Temperature dependence of reduced transverse and longitudinal ^{17}O relaxation rates and reduced angular frequencies of solutions containing $[Gd(Try\text{-}TTDA)(H_2O)]^{2-}$ at 9.4 T. (c = 0.020 mol kg^{-1}, pH = 7.4).

1000K/T	$\ln(1/T_{2r})$	$\ln(1/T_{1r})$	$\Delta\omega_r/10^6$ rad s^{-1}
3.595	14.368	11.715	–0.619
3.531	14.288	11.573	–0.719
3.411	14.064	11.302	–0.790
3.224	13.566	10.881	–0.770
3.047	12.988	10.482	–0.688
2.957	12.672	10.279	–0.646
2.872	12.364	10.087	–0.626

Table S3. Signal intensity of the T_1-weighted MR images of $[Gd(Try\text{-}TTDA)(H_2O)]^{2-}$ and metal ions in the molar ratio = 1:1.

Concentration (mM)	0.01	0.05	0.1	0.2
Cu(II)	1101±29	1532±54	1985±49	2073±67
La(III)	1108±40	1164±18	1181±55	1101±16
Mg(II)	1123±31	1306±26	1262±37	1106±24
Gd(III)	817±13	956±20	1121±17	1237±29

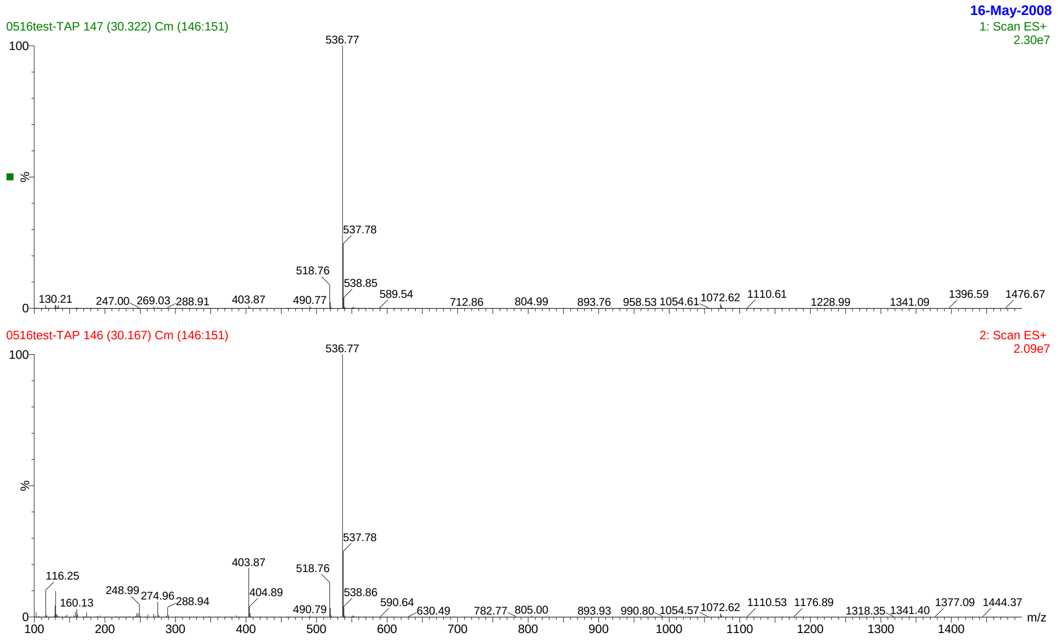

Fig. S1 ESI Mass spectrum of Try-TTDA.

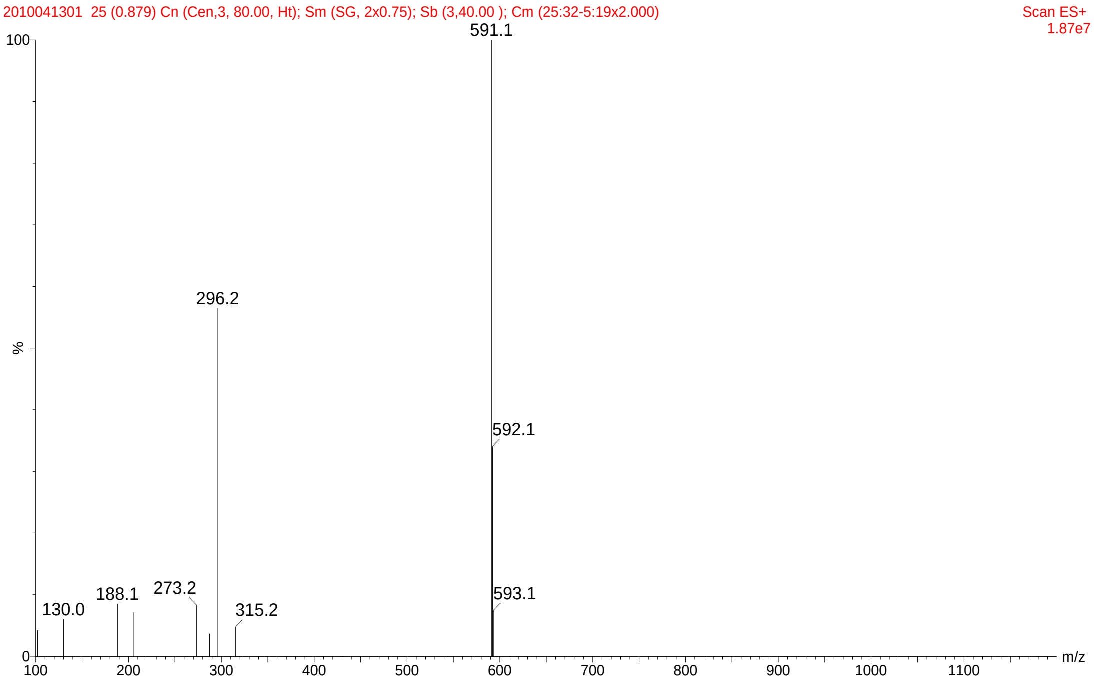

Fig. S2 ESI Mass spectrum of Try-ac-DOTA.

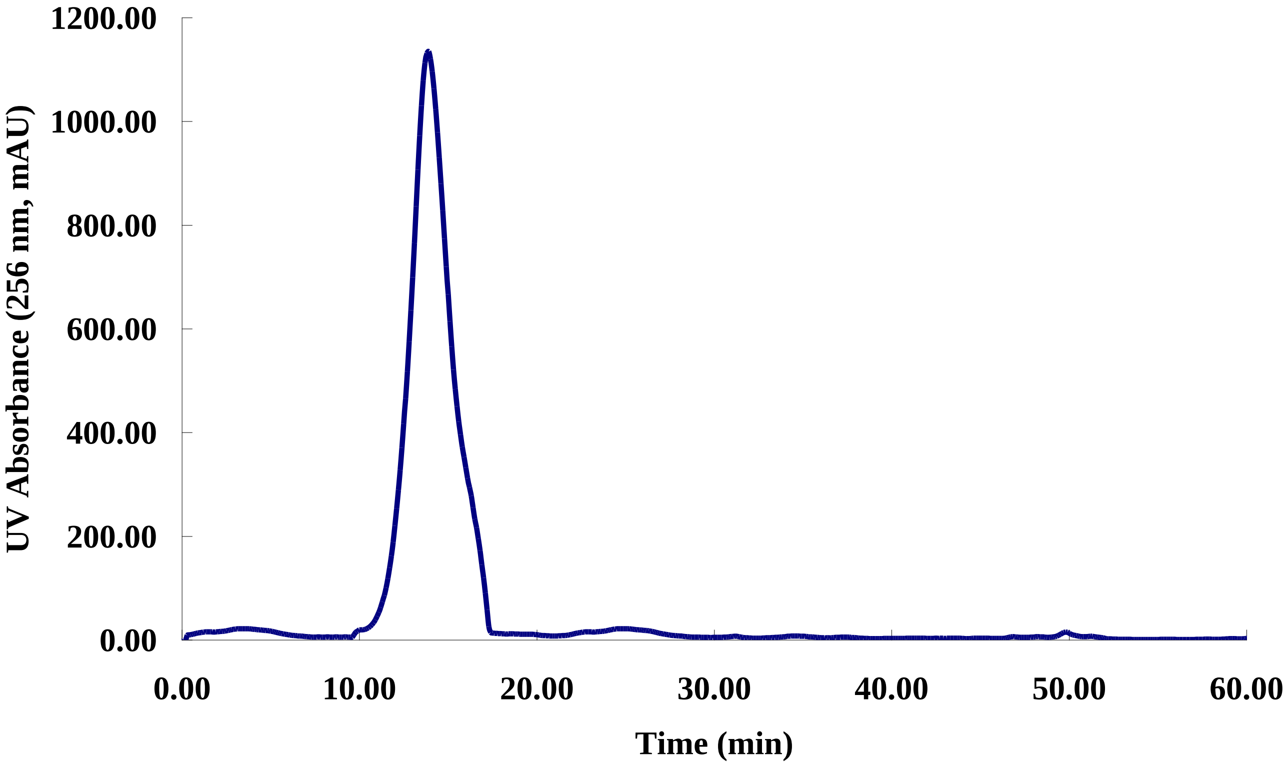

Fig. S3 HPLC chromatogram of the [Gd(Try-TTDA)(H_2O)]$^{2-}$ complex (PBS buffer, pH = 7.4 ± 0.1). One peak at 13.9 min was detected by UV detector at 256 nm (blue line) A Supelco RP-C18 column (5 μm, 4.6 × 250 mm) was used. One peak at 13.9 min ((MS ESI$^+$): *m/z*: 689.8[M+H]$^+$) was detected.

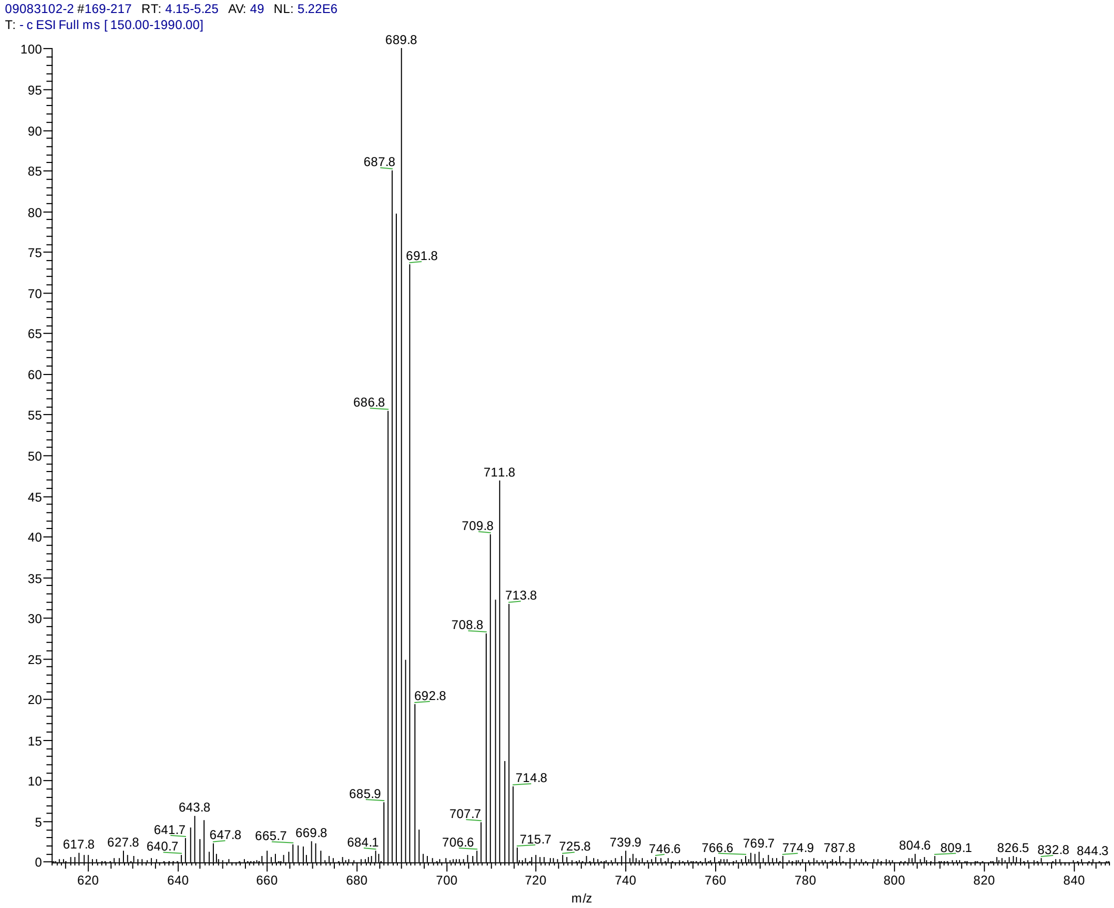

Fig. S4 ESI Mass spectrum of [Gd(Try-TTDA)(H_2O)]$^{2-}$ complex.

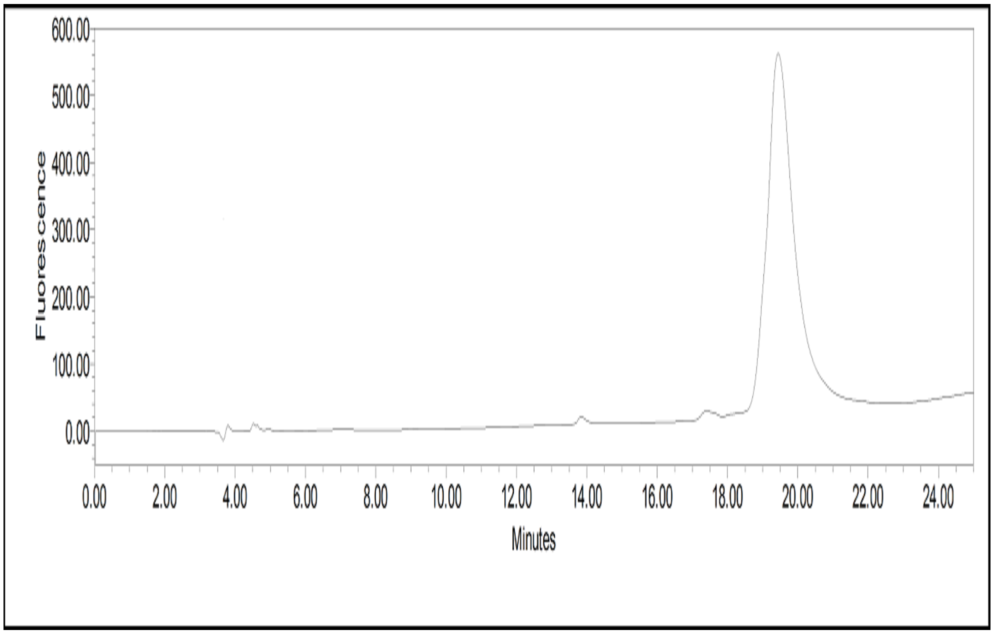

Fig. S5 HPLC chromatogram of the $[Gd(Try\text{-}ac\text{-}DOTA)(H_2O)]^-$ complex (PBS buffer, pH = 7.4 ± 0.1). One peak at 19.6 min was detected by RI detector at 256 nm. A Supelco RP-C18 column (5 μm, 4.6 × 250 mm) was used. One peak at 19.6 min ((MS ESI$^+$): *m/z*: 748.8$[M+3H]^+$) was detected.

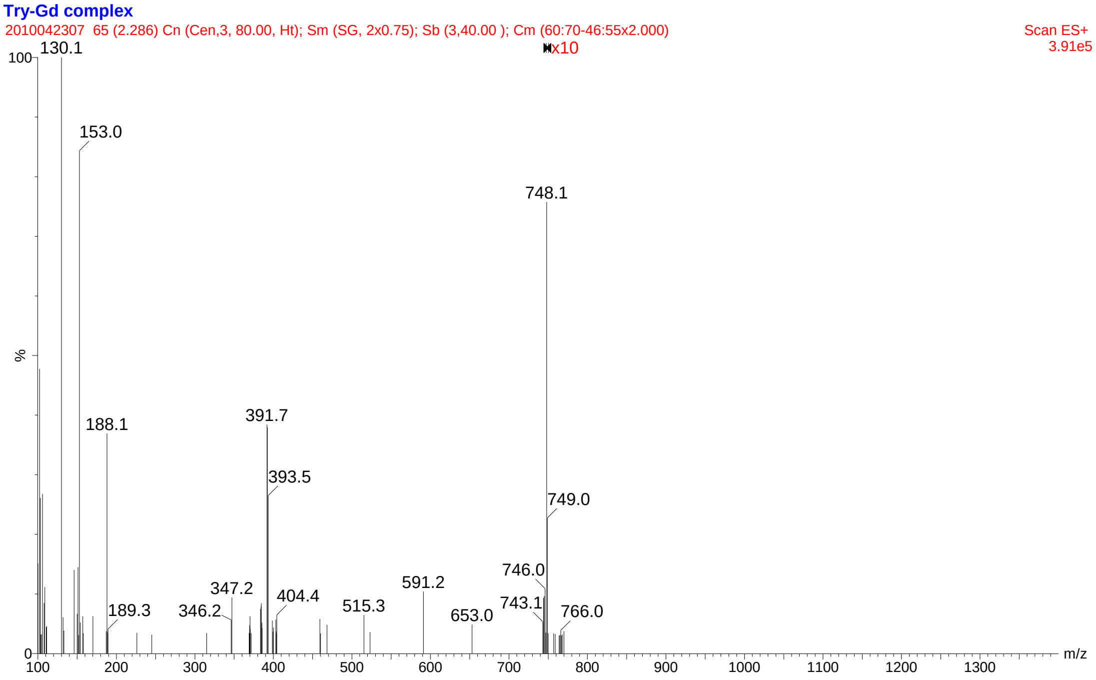

Fig. S6 ESI Mass spectrum of [Gd(Try-ac-DOTA)(H_2O)]$^-$ complex.

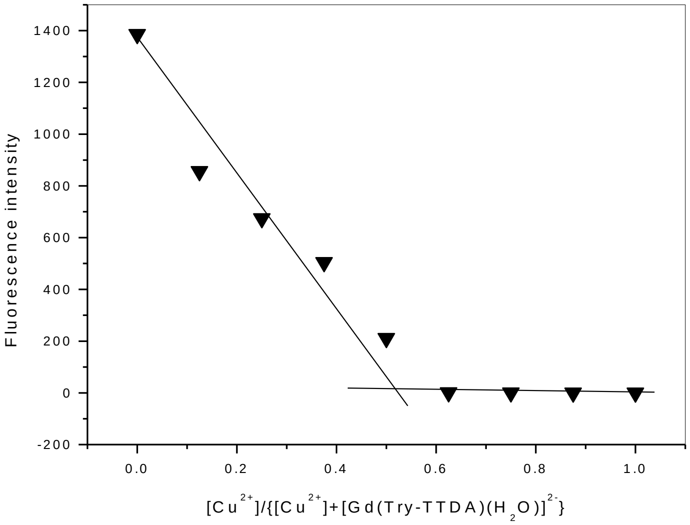

Fig. S7 Job's plot of $[Gd(Try\text{-}TTDA)(H_2O)]^{2-}$ interaction with Cu(II) obtained by fluorescence measurements (λ_{ex} = 281 nm, λ_{em} = 360 nm). The total concentration of $[Gd(Try\text{-}TTDA)(H_2O)]^{2-}$ and Cu(II) is 1.0 mM.

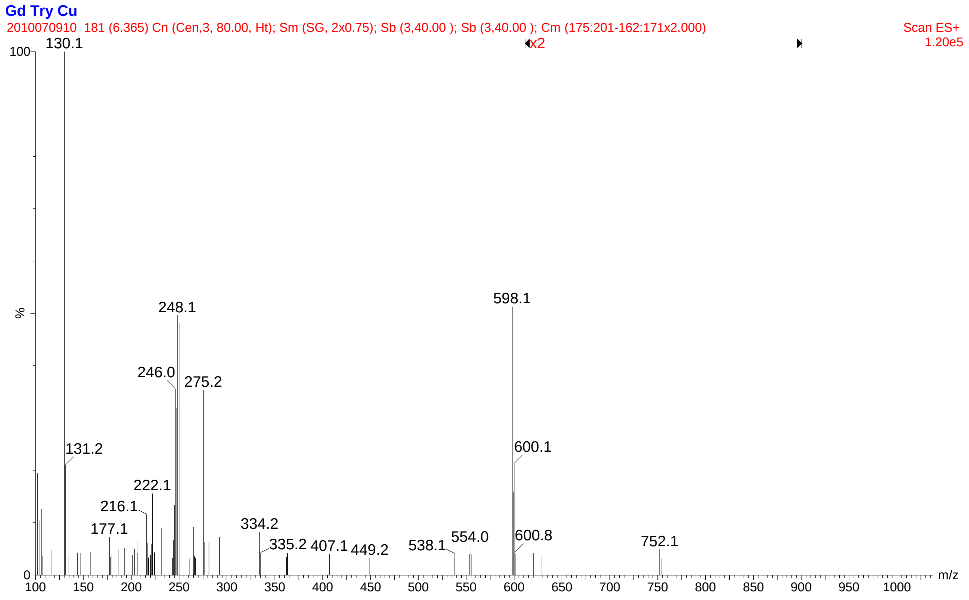

Fig. S8 ESI Mass spectrum of $[Gd(Try\text{-}TTDA)(H_2O)]^{2-}$ complex interaction with Cu(II).

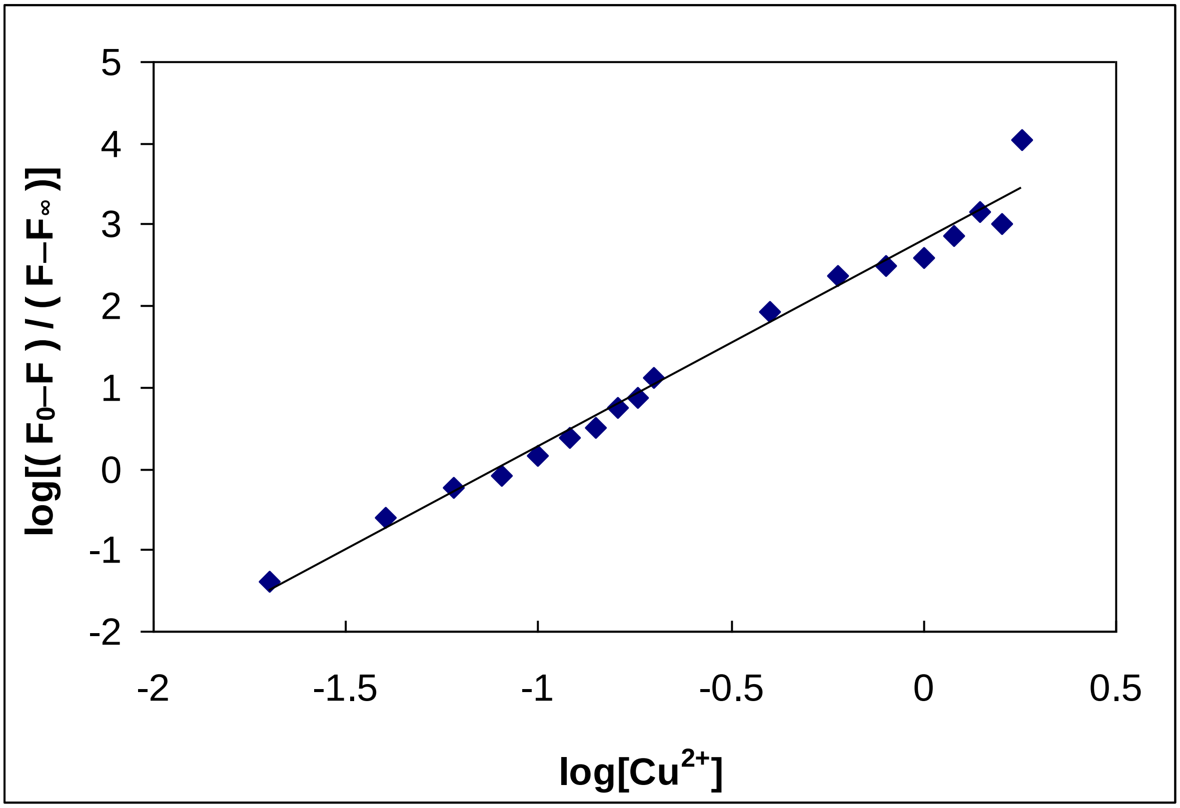

Fig. S9 Double-logarithmic plot of the quenching of fluorescence of $[Gd(Try\text{-}TTDA)(H_2O)]^-$ by the titration Cu^{2+}, where F_o, F and F_∞ are the relative fluorescence intensities of $[Gd(Try\text{-}TTDA)(H_2O)]^-$, $[Gd(Try\text{-}TTDA)(H_2O)]^-$ in the presence of a known concentration of Cu^{2+} and $[Gd(Try\text{-}TTDA)(H_2O)]^-$ saturated with Cu^{2+} (100 equivalents), respectively.

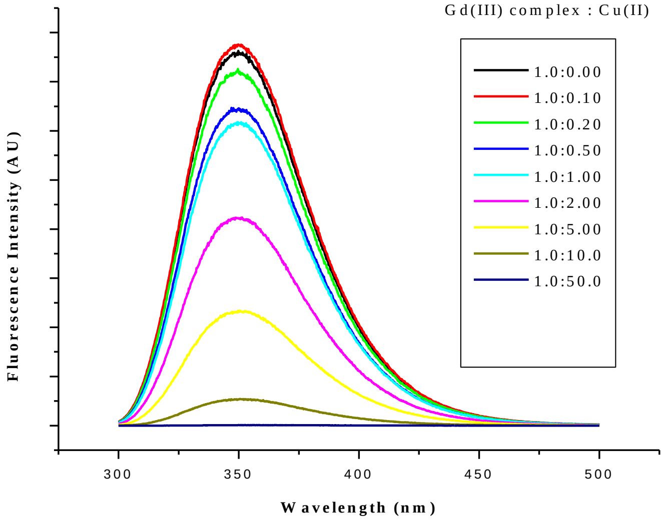

Fig. S10 Fluorescence emission spectra of 100 μM [Gd(Try-ac-DOTA)(H_2O)]$^-$ interaction with Cu(II), pH= 5.5 acetate buffer solution.

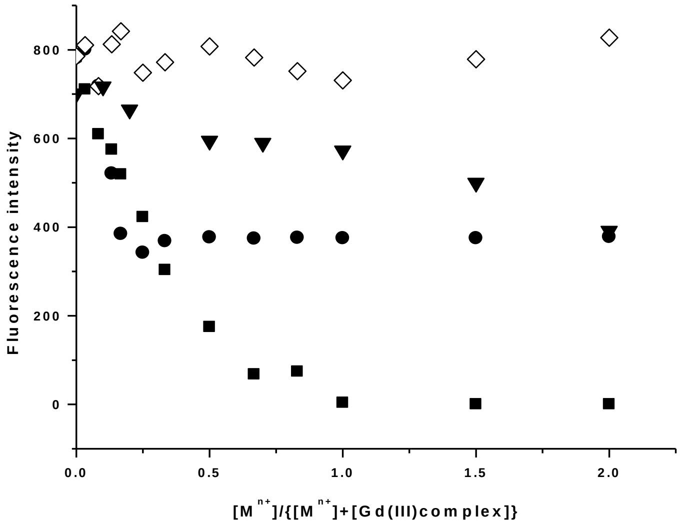

Fig. S11 Quenching plots of the fluorescence of Gd(III) complex against mole equivalents of metal ions added, Cu(II)(■), Mg(II)(◊), La(III)(●) for [Gd(Try-TTDA)(H$_2$O)]$^{2-}$ and Cu(II) **(▼)** for [Gd(Try-ac-DOTA)(H$_2$O)]$^{-}$, at 37.0 ± 0.1 °C and 20 MHz, pH 5.5 acetate buffer solution.